PHYSICAL REVIEW B VOLUME 39, NUMBER 1 1 JANUARY 1989

Gorsky-Bragg-Williams approach to the study of long-period superlattice phases in binary alloys

G. Ceder, M. De Graef, and L. Delaey
Department of Metallurgy and Materials Engineering, Catholic University Leuven, De Croylaan 2, B-3030 Heverlee, Belgium

J. Kulik
Lawrence Berkeley Laboratory, Materials and Chemical Sciences Division, Berkeley, California 94720
and Department of Materials Science and Mineral Engineering, University of California, Berkeley, California 94720

D. de Fontaine
Department of Materials Science and Mineral Engineering, University of California, Berkeley, California 94720
(Received 6 June 1988)

The influence of the shape of the reciprocal-space potential on the relative stability of long-period superlattice (LPS) phases in binary alloys is discussed in a Gorsky-Bragg-Williams approximation. First, for a certain class of LPS phases, the set of pair interaction parameters is reduced to a smaller set of parameters which characterize only the essential aspects of the reciprocal-space potential. Minimization of the free energy for different LPS phases is then used to extract some general tendencies, such as the change of wave vector towards the potential minimum (with increasing temperature) and the increasing stability of complex phases with deepening of the potential minimum.

I. INTRODUCTION

The past years have seen a rekindling of interest in long-period superstructures (LPS) in binary alloys due to the suggestion that Ising models with competing interactions, such as the axial next-nearest-neighbor Ising (ANNNI) model, could serve as useful theoretical paradigms in elucidating the thermodynamics of these systems.[1,2] The original qualitative explanation concerning the origin of these modulated structures was based on the interaction between the Fermi surface and the new Brillouin-zone boundaries resulting from the long-period modulation—a kind of ordering analog of the Peierls instability.[3] This explanation, although incomplete, is undoubtedly correct and has been placed on a more solid footing by recent work.[4] What is lacking from this argument, however, is a thermodynamic treatment of the long-range-ordered state, including the change of modulation wavelength with temperature and the tendency of many systems to lock in to commensurate phases, particularly at low temperatures. This behavior has been observed in a number of systems; examples include Ti_3Al,[5] Ag_3Mg,[6,7] Au_3Zn,[8] Cu_3Al,[9,10] and Cu_3Pd.[11,12] It is in this regard that Ising models become useful in illuminating the order-disorder behavior of these systems.

The ANNNI model is one model—a particularly simple one—which exhibits a rich variety of modulated phases.[13] There is, in fact, a striking resemblance between the so-called $\langle 2^m1 \rangle$ and $\langle 2^m3 \rangle$ phases (and their generalizations) predicted by the model and certain experimentally observed LPS phases in Ag_3Mg and Au_3Zn, respectively.[1,2] Consequently, there have been recent attempts to generalize the scheme of competing interactions employed in the ANNNI model to one more suitable for describing modulated ordered phases on close-packed lattices.[6,12,14] A phase diagram within the Gorsky-Bragg-Williams approximation has been calculated for one such generalization.[14]

The purpose of this paper is to consider further some generalizations of the ANNNI model to the fcc lattice. Specifically, for a certain class of modulated structures in alloys, the effect of a large set of competing pair interactions can be parametrized by a much smaller set of parameters $\{J_n\}$ analogous to the three parameters J_0, J_1, and J_2 used in the ANNNI model. The effect of these parameters on the relative phase stability will then be illustrated using the Gorsky-Bragg-Williams (GBW) approach.

II. THEORY

Since most alloys mentioned above can be regarded as LPS phases based on the $L1_2$ unit cell, only this cell will be considered in the following. Extension to other basic cells is straightforward.

The main point in this approach is that it is not necessary to know the complete reciprocal-space potential in order to describe the phase stability of a certain one-dimensional long-period superlattice phase; effectively, only the wave vectors for which the structure factor is different from zero are needed for a full description of the structure. This was also an assumption of the concentration wave method;[15] a particular ordered phase is described by a limited number of wave vectors. Hence, it is important to know the set of wave vectors that describes the complete structure.

Let the x axis coincide with the direction of modulation. We shall restrict our attention to LPS phases characterized by a one-dimensional modulation consisting of regularly spaced conservative antiphase boundaries

(APB) normal to the x axis. Furthermore, we shall neglect the contribution to the free energy of wave vectors of the form $(q,0,0)$ since these are often very weak. From structure-factor calculations,[16] it then follows that, apart from the superlattice wave vector (1,0,0), the only contributing wave vectors are of the type:

$$(\pm ng,1,0) \text{ and } (\pm ng,0,1) \text{ where } n \text{ is odd} , \quad (1)$$

$g=1/2M$ is the fundamental wave vector of the structure. For commensurate superlattices the average APB period M can be written as the ratio of two integers $M=P/Q$, P and Q being relative primes.[17,18] The total number of independent vectors is limited because only vectors belonging to the first Brillouin zone should be considered. The finite set of wave vectors in the first Brillouin zone can readily be deduced to be

$$ng=\frac{i}{P}, \quad i=0,1,\ldots,(P-1)/2 \text{ for } Q \text{ even} ,$$

$$ng=\frac{i}{2P}, \quad i=1,3,5,\ldots,P \text{ for } Q \text{ odd} .$$

According to Ref. 16 the internal energy per atom with respect to the disordered phase can be written as

$$E=\tfrac{1}{2}\sum_{\mathbf{k}} V(\mathbf{k})|\Gamma(\mathbf{k})|^2 . \quad (2)$$

Here $\Gamma(\mathbf{k})$ is the amplitude of a concentration wave with wave vector $\mathbf{k}$. The summation is carried out over the forementioned vectors and the superlattice vector (1,0,0). $\Gamma(\mathbf{k})$ are the Fourier transforms of the concentration deviation variables $\gamma_i=\langle c_i\rangle-c$, where c_i is the site concentration on site i (0 or 1) and c is the bulk concentration:

$$\Gamma(\mathbf{k})=\frac{1}{N}\sum_i \gamma_i \exp(-i2\pi\mathbf{k}\cdot\mathbf{r}_i) . \quad (3)$$

The total Helmholtz free energy in the Gorsky-Bragg-Williams approximation can be written as[14]

$$F=\tfrac{1}{2}\sum_{\mathbf{k}} V(\mathbf{k})|\Gamma(\mathbf{k})|^2 + \frac{kT}{N}\sum_{i=1}^{N}[c_i\ln c_i+(1-c_i)\ln(1-c_i)] . \quad (4)$$

Using (3) this equation can be written in terms of the concentration wave amplitudes $\Gamma(\mathbf{k})$; the $\Gamma(\mathbf{k})$'s can then be used as variables in a minimization routine to obtain the free energy for a certain phase.

The limited number of wave vectors and the fourfold crystal symmetry reduce the region of reciprocal space where the potential coefficients have to be computed to a line between (0,1,0) and (1/2,1,0) inside the first Brillouin zone. Along this line (k,1,0) the potential is parametrized as follows:

$$V(k)=J_0+2\sum_n J_n\cos(2\pi nk) . \quad (5)$$

The connection between the set of parameters $\{J_n\}$ and the pair interactions $V(\mathbf{r})$ is made as follows. The potential in reciprocal space $V(\mathbf{k})$ can be written

$$V(\mathbf{k})=\sum_{\mathbf{r}} V(\mathbf{r})\exp(-i2\pi\mathbf{k}\cdot\mathbf{r})=\sum_s V_s\phi_s , \quad (6)$$

where the function $\phi_s(k)$ is called the shell function for the sth coordination shell. The form of these functions has been given elsewhere.[6] The quantity V_s is the pair interaction parameter for shell s. Substituting the value $(k,1,0)$ for $\mathbf{k}$ one obtains the form given in Eq. (5) with the J_n expressed as linear combinations of the V_s.[12,19] Explicitly, for interaction parameters up to and including the 32nd shell, J_n for $n=0$–3 are given by

$$J_0=-4V_1+4V_2+4V_4-8V_5+4V_8-4V_{10}+8V_{11}-8V_{14}+4V_{17}-8V_{18}+4V_{20}+8V_{24}-8V_{29}-4V_{30}+8V_{32}+\cdots ,$$

$$J_1=V_2-4V_3+4V_4+4V_6-8V_7+4V_{11}-4V_{12}+8V_{13}-8V_{16}-8V_{21}-8V_{23}+4V_{24}+8V_{26}+\cdots ,$$

$$J_2=V_8-4V_9+4V_{11}+4V_{13}-8V_{15}+4V_{17}-4V_{19}+8V_{21}-8V_{25}+4V_{28}-8V_{31}+4V_{32}+\cdots ,$$

$$J_3=V_{20}-4V_{22}+4V_{24}+4V_{26}-8V_{27}+4V_{32}+\cdots .$$

The analysis is simplified considerably, then, since one need only parametrize the problem using the $\{J_n\}$ rather than the full set of $\{V_s\}$. The higher-order J_n terms become important only for increasingly larger interaction distances. Keeping only terms involving J_0, J_1, and J_2, one obtains the fcc analog of the ANNNI model but with

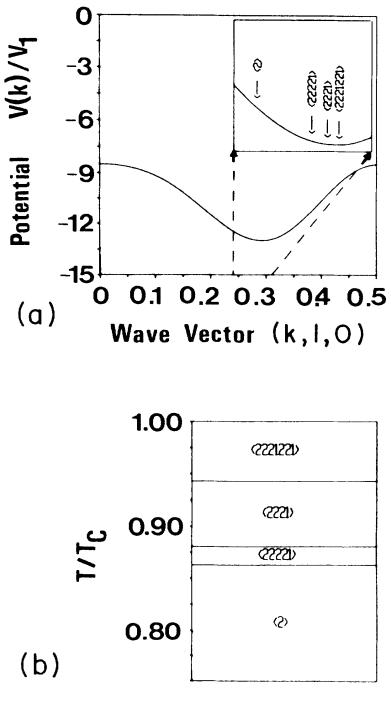

FIG. 1. (a) Reciprocal-space potential $V(k)/V_1$ along $(k,1,0)$; in the inset the fundamental wave vectors of four phases are indicated. (b) Stability domains of the $\langle 2\rangle$, $\langle 2^41\rangle$, $\langle 2^31\rangle$, and $\langle 2^312^21\rangle$ phases as a function of reduced temperature. ($J_0=-10.5653$, $J_1=0.3345$, $J_2=1.0326$, $J_3=-0.3345$.)

interactions retaining the full symmetry of the lattice (i.e., no anisotropy direction). It must be emphasized that implicit in this discussion is the assumption that the pair interactions $\{V_s\}$ are such that the extremum in $V(k)$ which occurs along the line from (0,1,0) to (1/2,1,0) is truly a minimum and not just a saddle point.

As in the ANNNI model, the ratio of the different J_n parameters will determine which phases are stable at different temperatures. In the following section results of a GBW computation of the free energy will be presented for different shapes of the potential function in reciprocal space; the effect of potential depth and position of the minimum on the relative stability of different LPS phases will be illustrated.

III. RESULTS

The shape of the potential curve $V(k)$ along the $(k,1,0)$ line strongly determines the stability domains of the different LPS phases and also the diffuseness of the antiphase boundaries. That this is so has already been suggested in previous work.[12,14] In this section the effect of a change of the potential depth and position of the minimum will be systematically analyzed, using an example potential. The composition will always be taken as A_3B.

A. Effect of the potential minimum

In Fig. 1(a) a potential curve is shown which is constructed in such a way that its minimum is at the fundamental wave vector ($q=1/2M$) of the $\langle 2^3 12^2 1\rangle$ phase: $q=0.2917$. The total free energy (4) was then minimized at different temperatures for this potential and the stability domains of the $\langle 2\rangle$, $\langle 2^4 1\rangle$, $\langle 2^3 1\rangle$, and $\langle 2^3 12^2 1\rangle$ phases are shown in Fig. 1(b). The latter phase is only stable at higher temperatures, despite the fact that the potential is minimal for the corresponding wave vector. At the lowest temperatures the $\langle 2\rangle$ phase is the most stable with $q=0.25$.

The stability of the $\langle 2\rangle$ phase with respect to the more complicated modulations can be explained from the fact that this phase is determined by only one wave vector; the absence of harmonics apparently influences the relative stability of the different phases. This can quite easily be deduced from the order parameters at different temperatures. The order parameters are defined as the normalized concentration wave amplitudes (the normalization factor being the concentration wave amplitude at zero temperature). In the following a graphical method will be employed to represent the order parameters for all harmonics: the order parameter is plotted as a hatched rectangle centered on the corresponding wave vector. The width of the rectangle is proportional to the concentration wave amplitude at zero temperature whereas the height represents the value of the normalized order parameter. Therefore, the area of each rectangle is proportional to $\Gamma(\mathbf{k})$; the square of the area is proportional to the contribution of each harmonic to the internal energy. This graphical method will now be used to illustrate the influence of temperature on the contributions of harmonics to the total stability of LPS phases.

In Fig. 2, the order parameters for the $\langle 2\rangle$ and $\langle 2^3 1\rangle$ phases are drawn for three different temperatures: $T=0$, $T=0.950T_c$, and $T=0.986T_c$. At $T=0$ [Fig. 2(a)] all order parameters are equal to unity. Despite the fact that the fundamental wave vector of the $\langle 2^3 1\rangle$ structure is closer to the potential minimum than that of the $\langle 2\rangle$ structure, the former one is less stable because of the large energy contributions of the different harmonics; i.e., the total "ordering-amplitude" is distributed over the fundamental and harmonic wave vectors. At higher temperatures [Fig. 2(b)] the entropy contribution to the free energy becomes increasingly important; the entropy will balance the large internal energy contributions of the harmonics which will hence decrease in amplitude. In Fig. 2(c) the situation close to the critical temperature T_c is

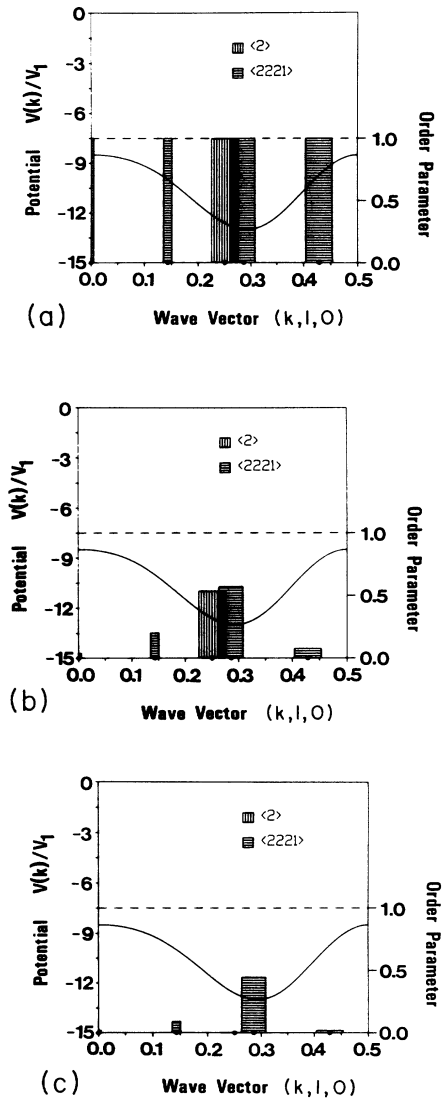

FIG. 2. Order parameters for the $\langle 2\rangle$ and $\langle 2^3 1\rangle$ phases at (a) $T=0$, (b) $T=0.950T_c$, and (c) $T=0.986T_c$ for the potential of Fig. 1(a). See text for more explanation.

shown: now the contributions of the different harmonics have decreased sufficiently to render the $\langle 2^3 1 \rangle$ structure more stable than the simpler $\langle 2 \rangle$ structure. The complete structure is now described by one sinusoidal concentration wave with fundamental wave vector $q = \frac{4}{14}$.

The vertical arrows in the inset of Fig. 1(a) indicate the positions of the fundamental wave vectors for the four computed structures in Fig. 1(b); as a function of temperature $q = 1/2M$ increases from $q = 0.25$ at $T = 0$ to $q = 0.2917$ which corresponds to the minimum of the potential curve. Hence, q changes towards the potential minimum at higher temperatures. In Fig. 3 the results of an analogous computation are represented for a potential for which the minimum lies at $q = 0.21875$ (corresponding to the $\langle 2^2 3 2^3 3 \rangle$ structure). In this case q decreases with increasing temperature. The general tendency derived from these computations suggests that with increasing temperature the most stable structure will come closer to the one corresponding with the minimum in the potential curve. This change of q does not have to be monotonous: it is possible that q first jumps over the potential minimum and then approaches it from the other side. This is illustrated in Fig. 4 where a potential is shown, constructed only with J_0, J_1, and J_2 with $J_2/J_1 = 0.55$. (Notice that in the ANNNI model this would correspond to a region close to the multiphase point $\kappa = 0.5$.) The minimum of this potential occurs at $q_{\min} = 0.325$. At low temperatures the wave vector $q = 0.25$; upon increasing the temperature, q first jumps to the other side of $q_{\min}$ ($\langle 21 \rangle$ phase) and then returns to the complex $\langle 2^2 1 (21)^3 \rangle$ phase with $q = 0.3214$.

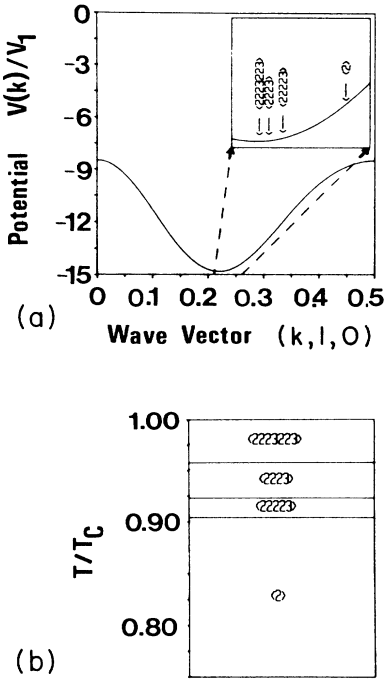

FIG. 3. (a) Reciprocal-space potential for $J_0 = -11.5227$, $J_1 = -0.3329$, $J_2 = 1.5113$, and $J_3 = 0.3329$; potential minimum at $q = 0.21875$. (b) Stability domains of the $\langle 2 \rangle$, $\langle 2^4 3 \rangle$, $\langle 2^3 3 \rangle$, and $\langle 2^3 3 2^2 3 \rangle$ phases.

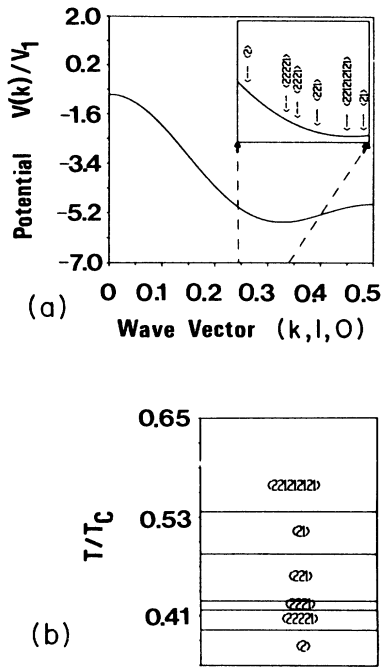

FIG. 4. (a) Reciprocal-space potential for $J_0 = -4.0$, $J_1 = 1.0$, and $J_2 = 0.55$. (b) Stability domains of a set of computed phases. Note that the wave vector jumps from one side of the minimum to the other.

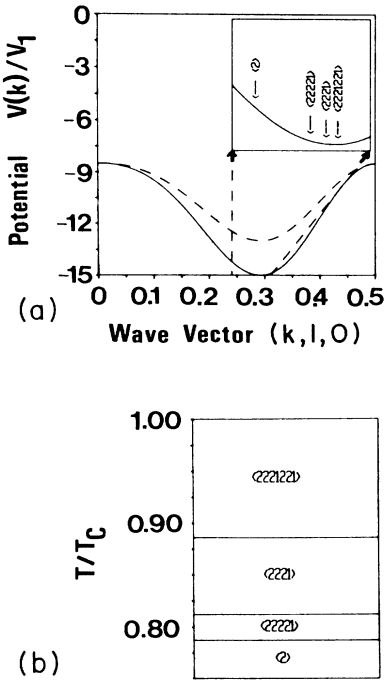

FIG. 5. Reciprocal-space potential with the same minimum position as in Fig. 1(a) (indicated with a dashed line) but with a deeper minimum. ($J_0 = -11.4832$, $J_1 = 0.4832$, $J_2 = 1.4916$, $J_3 = -0.4832$.) (b) Stability domains are wider for the more complex phases when compared with the stability diagram in Fig. 1(b).

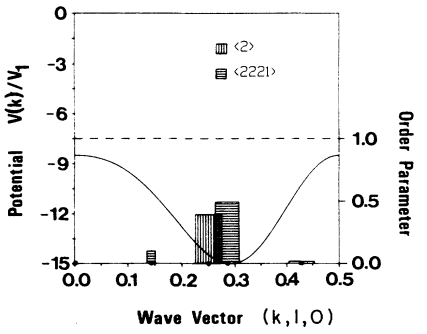

FIG. 6. Order parameters for the potential of Fig. 5(a) at $T=0.950T_c$. Compared with Fig. 2(b) the $\langle 2^31 \rangle$ phase is now more stable with respect to the $\langle 2 \rangle$ phase.

B. Effect of potential depth

Increasing the potential depth of, e.g., the potential in Fig. 1(a) and keeping the minimum at a constant position, one obtains the potential in Fig. 5(a). The minimum is 15% deeper than the previous potential (which is indicated with a dashed line). From the stability diagram in Fig. 5(b) it can be seen that a lowering of the potential well increases the stability domain of the more complex phases; the $\langle 2^312^21 \rangle$ structure now is stable at a lower relative temperature. This suggests that in the limit of infinite potential depth this phase will be stable from $T=0$ on. In Fig. 6 the order parameters are drawn for the $\langle 2 \rangle$ and $\langle 2^31 \rangle$ phases at $T=0.950T_c$; this is to be compared with Fig. 2(b). The internal energy contribution of the harmonics of the $\langle 2^31 \rangle$ phase are smaller for the lowest potential and this phase is also becoming more stable with respect to the $\langle 2 \rangle$ phase.

IV. CONCLUSIONS

In this paper the influence of the potential shape along the $(k,1,0)$ line in reciprocal space is analyzed; all minimizations were carried out using a Gorsky-Bragg-Williams approach for the free-energy computations. It should be emphasized that this approach will overestimate, in general, the critical transformation temperature T_c; however, it may give important qualitative information about the relative stability of different phases. The following conclusions can be made.

(1) Complex structures cannot be stable at low temperatures because of the contributions of the harmonic concentration waves.

(2) At high temperatures the structure with the wave vector at the potential minimum is the most stable structure; it is described by a single concentration wave which implies a sinusoidal modulation. This explains why the original Sato and Toth model,[3] derived at $T=0$ K, is actually valid at high temperatures only.

(3) Increasing the potential depth at the minimum position increases the stability domain of the more complex structures with $q=1/2M$ close to the minimum.

The harmonics of the concentration profile start disappearing already at low temperatures. Therefore, it is very likely that real alloy systems which show almost sinusoidal modulations at high temperatures (such as Cu_3Pd) probably have a rather deep minimum in the potential curve. For Cu-Pd alloys this potential curve has recently been derived from first-principles calculations[4] and it indeed shows a rather deep minimum. For the Ag-Mg system on the other hand, APB's are very sharply defined and therefore even at high temperatures the harmonic contributions to the concentration profile will still be substantial. An important parameter in this respect is the ratio $[V(k_{\min})-V(0)]/V(k_{\min})$ which characterizes the relative depth of the potential; the smaller this parameter the more important harmonic contributions will be at high temperatures.

ACKNOWLEDGMENTS

This research was carried out in the framework of the interuniversity networks for fundamental research financed by the Belgian Government (Contract No. UIAP 4). Work at Berkeley was supported by the Director, Office of Basic Energy Sciences, Materials Sciences Division of the U.S. Department of Energy under Contract No. DE-AC03-76SF00098. G.C. thanks the University of California for additional financial support.

[1]J. Kulik and D. de Fontaine, Mat. Res. Soc. Symp. Proc. **21**, 225 (1984).
[2]D. de Fontaine and J. Kulik, Acta Metall. **33**, 145 (1985).
[3]H. Sato and R. S. Toth, Phys. Rev. **127**, 469 (1961).
[4]G. M. Stocks *et al.*, Mat. Res. Soc. Symp. Proc. **81**, 15 (1987).
[5]A. Loiseau, G. Van Tendeloo, R. Portier, and F. Ducastelle, J. Phys. (Paris) **46**, 595 (1985).
[6]J. Kulik, S. Takeda, and D. de Fontaine, Acta Metall. **35**, 1137 (1987).
[7]Y. Fujino *et al.*, Phys. Rev. Lett. **58**, 1012 (1987).
[8]G. Van Tendeloo and S. Amelinckx, Phys. Status Solidi A **43**, 553 (1977).
[9]D. Broddin *et al.*, Micron Microsc. Acta **18**, 239 (1987).
[10]D. Broddin *et al.*, Philos. Mag. (to be published).
[11]D. Broddin *et al.*, Philos. Mag. **57**, 31 (1988).
[12]S. Takeda, J. Kulik, and D. de Fontaine, J. Phys. F **18**, 1387 (1988).
[13]See, for example, the review of P. Bak, Rep. Prog. Phys. **45**, 587 (1982).
[14]J. Kulik and D. de Fontaine, J. Phys. C **21**, L291 (1988).
[15]A. G. Khatchaturyan, Phys. Status Solidi B **60**, 9 (1973).
[16]D. Van Dyck, D. Broddin, J. Mahy, and S. Amelinckx, Phys. Status Solidi A **103**, 357 (1987).
[17]D. de Fontaine, Solid State Phys. **34**, 73 (1979).
[18]J. Kulik, S. Takeda, and D. de Fontaine (unpublished).
[19]J. Kulik, Ph.D. thesis, University of California at Berkeley, 1987.